The Secondary Structure in Solution of Acyl-Coenyzme A Binding Protein from Bovine Liver Using ^{1}H Nuclear Magnetic Resonance Spectroscopy†

Kim V. Andersen, Svend Ludvigsen, Susanne Mandrup,‡ Jens Knudsen,‡ and Flemming M. Poulsen*

Department of Chemistry, Carlsberg Laboratory, Gamle Carlsberg Vej 10, DK-2500 Copenhagen Valby, Denmark, and Institute of Biochemistry, University of Odense, DK-5230 Odense M., Denmark

Received May 16, 1991; Revised Manuscript Received August 22, 1991

ABSTRACT: Acyl-coenzyme A binding protein from bovine liver and the protein expressed in *Escherichia coli* by the recombinant gene of this protein have been studied by two-dimensional ^{1}H nuclear magnetic resonance spectroscopy. This protein has, in addition to the ability to bind acyl-coenzyme A, been reported to have several important physiological and biochemical functions. It is known as the diazepam binding inhibitor, as a putative neurotransmitter, as a regulator of insulin release from pancreatic cells, and as a mediator in corticotropin-dependent adrenal steroidogenesis. The only difference between the protein produced by recombinant techniques and the native acyl-coenzyme A binding protein is the N-terminal acetyl group present only in the native protein. The two proteins have 86 amino acid residues and a molecular mass of approximately 10000 Da. Complete assignment of the ^{1}H nuclear magnetic resonances has been obtained for a major proportion of the amino acid residues (55 residues), and partial assignment has been achieved for the others (31 residues). Sequential nuclear Overhauser effects have demonstrated that the protein has a secondary structure consisting of four α-helices of residues 1–15, 22–35, 52–60, and 68–85. Furthermore, a large number of long-range nuclear Overhauser effects have been identified, indicating that the assignment given here will provide a basis for a structure determination of this protein in solution by nuclear magnetic resonance spectroscopy.

Acyl-coenzyme A binding protein, ACBP,[1] is a small protein first discovered in bovine liver (Mogensen et al., 1987). ACBPs that are homologous and have very similar amino acid sequences have been isolated from rat, murine, porcine, bovine, and human sources (Knudsen, 1991). ACBP from birds and reptiles also shows a very strong homology with the mammalian ACBPs (Knudsen et al., unpublished data). The common existence of these homologous proteins among higher organisms in the taxonomic system and the conservation of the amino acid sequence suggest that this protein has one or several important physiological functions. The finding that the protein binds acyl-coenzyme A gives the protein a potential role in acyl-coenzyme A metabolism (Rasmussen et al., 1990); however, it has been suggested that the protein also has neurotransmitter activity, as the sequence of the rat and bovine brain diazepam-binding inhibitor is identical with those of the rat and bovine ACBP, respectively (Knudsen & Nielsen, 1990). Other studies have shown that the protein may play a role in the regulation of insulin release from the porcine isles of Langerhans (Chen et al., 1988) and that the protein may have a role as mediator in corticotropin-dependent adrenal steroidogenesis (Besman et al., 1989). These reports suggest that the protein could be a multifunctional protein with indeed very important physiological and biochemical roles.

The present work is the first in a series of NMR studies that have the purpose to determine the three-dimensional structure of bovine ACBP in solution and the structure of the complex between the ligand, acyl-coenzyme A, and ACBP, including the location of the binding site in ACBP. In order to accomplish this, we have studied both the native protein from bovine liver and the protein expressed by the recombinant ACBP gene in *E. coli* strains (Mandrup et al., 1991). Here we report the sequence-specific assignment of the NMR spectra of these two proteins and the secondary structure that has been determined on the basis of these assignments, sequential NOEs, and measurements of the $^3J_{H^NH^\alpha}$ coupling constants. Furthermore, an outline of the three-dimensional structure has been constructed on the basis of the long-range NOEs observed in spectra of ACBP.

It is the ultimate purpose of these studies to produce a structural platform for the studies that have so far suggested the multifunctionality of this protein.

Materials and Methods

Native bovine ACBP and recombinant ACBP were prepared and purified as described previously (Mikkelsen et al., 1987; Mandrup et al., 1991). All chemicals used were analytical grade. Deuterium oxide was purchased from Merck. NMR samples were prepared by dissolving lyophilized protein in 0.6 mL of 90:10 $H_2O/^2H_2O$ or 99.96% ^2H_2O and adjusting the pH or p^{2}H; in both cases the pH-meter readings were recorded and no correction for deuterium effects were applied. Typically, protein concentrations for native ACBP were between 1 and 4 mM and for recombinant ACBP between 5 and 10 mM.

NMR spectra were recorded on a Bruker AM500 NMR spectrometer equipped with an Aspect 3000 computer. The following two-dimensional NMR experiments were performed: NOESY (Jeener et al., 1979; Anil-Kumar et al., 1980; Anil-Kumar et al., 1981; States et al., 1982), COSY (Aue et

† This work was supported by the Carlsberg Foundation (KVA) and the Natural Science Foundation of Denmark.

* To whom correspondence should be addressed.

‡ University of Odense.

[1] Abbreviations: NOESY, two-dimensional nuclear Overhauser enhanced spectroscopy; COSY two-dimensional correlated spectroscopy; 2QF, double-quantum filtered; TOCSY, total correlation spectroscopy; 2QS, double-quantum spectroscopy; ACBP, acyl-coenzyme A binding protein.

0006-2960/91/0430-10654$02.50/0 © 1991 American Chemical Society

al., 1976; Marion & Wüthrich, 1983, 1983; Neuhaus et al., 1985), 2QF–COSY (Piantini et al., 1982; Rance et al., 1983), relayed COSY (Eich et al., 1982; Wagner, 1983), 2QS (Boyd et al., 1983; Braunschweiler et al., 1983; Wagner & Zuiderweg, 1983), and TOCSY (Braunschweiler & Ernst, 1983; Bax et al., 1985; Griesinger et al., 1988). In all cases the spectra were recorded and transformed using the hypercomplex two-dimensional Fourier transform yielding quadrature detection and pure phase (Bachmann et al., 1977; States et al., 1982). The experimental details concerning these NMR experiments were as described previously (Kjær et al., 1987).

The $^3J_{H^NH^\alpha}$ coupling constants were measured as described by Ludvigsen et al. (1991) using a combined analysis of NOESY and COSY spectra. NOEs were assigned using the list of sequence-specific assignments. Data were processed on a Stardent 1500 computer using software developed in-house. Phase-sensitive Fourier transformations were used in all cases. Spectra were zero-filled to yield final spectral matrices of 2048 complex points in ω_1 and 4096 complex points in ω_2. Window functions such as shifted sine bells, exponential multiplication, and Gaussian multiplication were used to enhance the analysis of the spectra. Some spectra were corrected for a distorted baseline in ω_2 using third-order Legendre polynomials.

The protein assignment program Pronto (Kjær et al., 1991) was used as a computer-driven assignment tool and a complete data base including catalogs of all the assigned spin systems was generated in order to make a record of the assignment process.

Results

The assignments of the NMR spectrum of ACBP was based on the analysis of a set of two-dimensional ^{1}H NMR spectra including NOESY, COSY, relayed COSY, TOCSY, and 2QS spectra all recorded at pH 7.0 at 298 K both of the ACBP and of recombinant ACBP. The protein unfolds reversibly at low pH at room temperature, the solubility is rather low at pH close to the isoelectric point of 5.9, and the samples are not fit for lengthy NMR analysis at temperatures at and above 310 K. Therefore, the present study is primarily based on studies at only one set of conditions as described above. Under these conditions, the amide hydrogen solvent exchange is relatively fast, and this has to some extent hampered the assignment process. The methods of assignments have followed very closely the guidelines already well established in studies of many other proteins in the size range up to 10000 Da (Wüthrich, 1986).

The Fingerprint Region

The fingerprint region of the COSY spectrum of the native ACBP contains 79 readily observable H^N–H^α cross peaks of which five pairs of the characteristic glycine H^N–H^α cross peaks were readily identified (see later). An additional set of two H^N–H^α resonances were identified at H^α chemical shifts near the water resonance in 2QS spectra recorded without water suppression. Recording of the recombinant ACBP 2QF-COSY spectra at higher concentrations, up to 10 mM, improved the signal-to-noise ratio sufficiently to detect the remaining very weak H^N–H^α cross peaks (Figure 1). Of the total number of 78 non-glycine H^N–H^α couplings in the recombinant ACBP, 75 were identified in the spectra, missing out the cross peaks of Gln2, Ile39, and Asp48. The H^N–H^α cross peak of Asp48 was identified in a 2QS spectrum recorded without water suppression. In the spectra of native ACBP, the H^N–H^α cross peak of the N-acetylated Ser1 was present, and the H^N–H^α cross peak of Gln2 was observed. The latter was not seen in the recombinant ACBP. In the spectra of the native ACBP, H^N–H^α cross peaks were not observed for Leu15, Asp21, Tyr28, Asp48, and Lys62. In the fingerprint region of the recombinant and the native proteins, NMR spectra show a very high degree of similarity; however, some differences were observed for a number of H^N–H^α cross peaks (Tables I and II). The sequential assignments later showed that many of these differences were in residues in the N-terminal part and the C-terminal part of the protein which are both forming α-helices. Other chemical shift differences of the ^{1}H resonances in the peptide backbone were seen in other regions of the amino acid sequence, suggesting that these regions are also perturbed by the electrostatic effects present when the N-terminal amino group is not acetylated.

Amino Acid Spin System Assignments

Glycines (Gly37, Gly45, Gly51, Gly63, and Gly85). The five glycines were identified from their H^N–($H^{\alpha1}$ + $H^{\alpha2}$) cross peaks in the 2QS spectrum in H_2O (Figure 2), and subsequently the characteristic glycine cross peaks in the fingerprint region of the COSY spectrum were identified.

Alanines (Ala3, Ala8, Ala9, Ala20, Ala34, Ala53, Ala57, Ala69, and Ala72). The nine alanines were unambiguously assigned by combining the information in the COSY and the TOCSY spectra as seen in Figure 3. Minor chemical shift differences were observed for three alanines, Ala 3, Ala 8, and Ala 9, in the two forms of ACBP, in particular, those of their amide protons.

Threonines (Thr17, Thr35, Thr41, and Thr64). The H^α, H^β, and the $H^{\gamma2}$ of the four threonines were assigned from the COSY and TOCSY spectra. For Thr35 and Thr64, the $H^{\gamma1}$ of the hydroxy group which is not normally seen in protein NMR spectra of threonyl residues was observed at 4.459 and 5.896 ppm, respectively, by the coupling to the H^β. This suggests that the hydrogens of the two hydroxyl groups are not in fast exchange with the aqueous solvent and possibly engaged in a hydrogen bond.

Valines (Val12, Val36, and Val177). The H^βs of the three valines are only separated by 0.042 ppm. The TOCSY connectivity between the H^α and the methyl H^γs was only clearly observed in the spectra of the recombinant ACBP (Figure 4). The three H^α–H^β cross peaks were all observed in both COSY and TOCSY spectra.

Isoleucines (Ile27, Ile39, Ile74, and Ile86). The H^N–H^α cross peak of Ile39 was not observed in the fingerprint region of either the recombinant or the native ACBP NMR spectra. However, the position of the H^N was established from NOE spectra. Otherwise the assignment of the spin systems was straightforward; however, the assignment of the ethyl part of one isoleucine, which was later found to be Ile74, has so far not been accomplished. The Ile39 spin system chemical shifts are characteristic of a ring current shifted isoleucine residue very close to one or several aromatic residues.

Leucines (Leu15, Leu25, Leu47, Leu61, and Leu80). The pairs of the isopropyl methyl groups of the five leucines could be distinguished from those of the valines only after the unambiguous assignment of the three valine spin systems. The differences in chemical shifts of the valine H^βs and four of the leucine H^γs assisted these assignments. The entire spin system of Leu 15 was only fully detected in the recombinant ACBP; in native ACBP the H^N–H^α cross peak of this spin system has not been observed.

Aromatic Residues (Tyr28, Tyr31, Tyr73, and Tyr84; Phe5, Phe26 and Phe49; Trp55 and Trp58). The assignment of the spin systems of the benzenoid part of the aromatic side chains in phenylalanines, tyrosines, and tryptophans was obtained from the set of COSY, relayed COSY, and TOCSY spectra

Table I: ^{1}H Chemical Shifts ±0.002 in Recombinant ACBP at pH 7.0 and 298 K[a]

residue	H^N	H^α	H^β	others
1 Ser		4.099	4.188, 4.027	
2 Gln				2.463 (H^γ); 8.262, 6.577 ($H^{\epsilon 2}$)
3 Ala	8.558	4.286	1.462	
4 Glu	8.042	4.067	2.357, 2.297	
5 Phe	8.401	4.260	3.376, 3.102	7.206 (H^δ); 6.491 (H^ϵ); 6.366 (H^ζ)
6 Asp	8.902	4.268	2.762, 2.679	
7 Lys	7.768	4.167	2.006, 1.906	
8 Ala	8.061	4.325	1.704	
9 Ala	8.409	4.816	1.215	
10 Glu	7.429	4.298	2.199, 2.199	
11 Glu	8.506	3.948	2.276, 1.699	2.448, 2.707 (H^γ)
12 Val	8.147	3.646	2.219	0.926, 1.040 (H^γ)
13 Lys	7.103	3.992	1.457, 1.601	
14 His	7.971	4.745	3.565, 3.028	7.358 ($H^{\delta 2}$); 8.154 ($H^{\epsilon 1}$)
15 Leu	6.914	4.706	1.777, 1.583	2.094 (H^γ); 1.019, 0.878 (H^δ)
16 Lys	8.475	3.954	1.933	
17 Thr	7.122	4.283	3.803	1.147 ($H^{\gamma 2}$)
18 Lys	7.889	4.263	1.662	
19 Pro		3.881	2.353, 1.683	1.519, 1.781 (H^γ); 3.428, 4.037 (H^δ)
20 Ala	8.189	4.361	1.574	
21 Asp	9.120	4.320	2.685, 2.622	
22 Glu	9.583	4.136	2.133	2.420 (H^γ)
23 Glu	7.085	4.214	2.704, 2.132	1.847 (H^γ)
24 Met	8.304	4.421	2.261, 2.230	2.743, 2.460 (H^γ)
25 Leu	8.574	4.278	2.052, 1.562	1.883 (H^γ); 0.993, 0.871 (H^δ)
26 Phe	7.863	4.356	3.640, 3.325	7.088 (H^δ); 7.008 (H^ϵ); 6.874 (H^ζ)
27 Ile	8.418	4.083	2.496	1.106 ($H^{\gamma 2}$); 1.388, 1.773 ($H^{\gamma 1}$); 0.503 (H^δ)
28 Tyr	8.927	4.260	3.019, 3.434	7.049 (H^δ); 6.873 (H^ϵ)
29 Ser	8.456	3.320	4.001, 3.700	5.011 ($O^\gamma H$)
30 His	8.189	3.850	3.422, 3.163	6.888 ($H^{\delta 2}$)
31 Tyr	8.675	3.673	3.059, 3.470	6.523 (H^δ); 6.575 (H^ϵ)
32 Lys	7.652	3.201	0.143, −0.661	0.538, −0.045 (H^γ); 0.792, 1.128 (H^δ); 2.476 (H^ϵ)
33 Gln	7.943	4.121	1.420	2.376 (H^γ)
34 Ala	7.607	3.989	0.850	
35 Thr	7.128	4.084	3.898	0.721 ($H^{\gamma 2}$); 4.459 ($H^{\gamma 1}$)
36 Val	8.543	3.901	2.203	1.060, 0.997 (H^γ)
37 Gly	7.797	4.326, 3.999		
38 Asp	8.150	4.468	2.508, 2.469	
39 Ile	8.236	2.264	−0.567	0.377 ($H^{\gamma 2}$); 0.063, −0.516 ($H^{\gamma 1}$); −0.806 (H^δ)
40 Asn	6.671	4.767	2.581, 3.119	6.471, 7.552 ($H^{\delta 2}$)
41 Thr	7.128	4.745	4.509	1.404 ($H^{\gamma 2}$)
42 Glu	8.731	4.331	1.882, 1.831	2.263 (H^γ)
43 Arg	8.163	2.370	0.902, −0.154	1.269, 0.620 (H^γ); 2.833, 2.605 (H^δ)
44 Pro	–	4.329	2.528, 1.807	1.858, 1.623 (H^γ); 2.891, 3.652 (H^δ)
45 Gly	8.329	4.006, 3.752		
46 Met	8.106	3.968	2.079, 2.009	2.574 (H^γ)
47 Leu	8.200	4.156	1.622	1.597 (H^γ); 0.932, 0.896 (H^δ)
48 Asp	7.527	4.771	2.998, 2.407	
49 Phe	7.734	4.175	3.255, 3.126	7.340 (H^δ); 7.476 (H^ϵ); 7.402 (H^ζ)
50 Lys	8.838	4.139	1.789	
51 Gly	8.198	3.907, 3.854		
52 Lys	8.736	3.907	1.857, 1.332	
53 Ala	7.693	4.340	1.575	
54 Lys	7.595	3.822	1.668	0.632, 1.536 (H^γ); 1.169, 0.995 (H^δ)
55 Trp	8.101	4.343	3.519, 3.297	7.087 ($H^{\delta 1}$); 9.218 ($H^{\epsilon 1}$); 7.367 ($H^{\zeta 2}$); 7.008 ($H^{\eta 2}$); 7.134 ($H^{\zeta 3}$); 8.033 ($H^{\epsilon 3}$)
56 Asp	9.381	4.537	2.961, 2.869	
57 Ala	7.907	4.275	1.731	
58 Trp	8.078	4.630	3.589, 3.043	7.514 ($H^{\delta 1}$); 9.936 ($H^{\epsilon 1}$); 7.095 ($H^{\zeta 2}$); 7.181 ($H^{\eta 2}$); 7.146 ($H^{\zeta 3}$); 7.592 ($H^{\epsilon 3}$)
59 Asn	9.358	3.749	2.567, 1.448	6.623, 7.835 ($H^{\delta 2}$)
60 Glu	7.729	4.004	2.159	
61 Leu	7.495	4.253	1.200, 2.001	1.760 (H^γ); 0.523, 0.004 (H^δ)
62 Lys	7.211	4.120	1.849, 1.620	1.309 (H^γ)
63 Gly	10.032	4.401, 3.776		
64 Thr	8.311	4.324	4.055	1.484 ($H^{\gamma 2}$); 5.896 ($H^{\gamma 1}$)
65 Ser	9.900	4.357	4.379, 4.173	
66 Lys	8.934	3.905	1.780	
67 Glu	8.818	3.947	2.054, 1.968	2.444 (H^γ)
68 Asp	8.021	4.540	2.863, 2.658	
69 Ala	8.534	4.295	1.427	
70 Met	8.611	3.823	2.175, 1.885	2.429, 1.401 (H^γ)
71 Lys	7.787	4.087	2.030	1.611 (H^γ)
72 Ala	7.876	4.308	1.613	
73 Tyr	8.538	3.932	3.785, 3.166	7.025 (H^δ); 6.772 (H^ϵ)
74 Ile	8.726	3.418	2.023	1.080 ($H^{\gamma 2}$)
75 Asp	8.386	4.362	2.768, 2.634	
76 Lys	8.041	4.108	1.887	
77 Val	8.603	3.320	2.177	1.008, 0.589 (H^γ)

Table I (Continued)

residue	H^N	H^α	H^β	others
78 Glu	8.331	4.018	2.213, 2.135	2.471, 2.471 (H^γ)
79 Glu	7.780	4.000	2.288, 2.317	1.989 (H^γ)
80 Leu	8.924	4.054	2.109	2.169 (H^γ); 0.887, 0.774 (H^δ)
81 Lys	9.013	3.696	1.878	1.252 (H^γ)
82 Lys	7.361	4.009	1.885, 1.422	
83 Lys	7.784	3.882	1.455, 1.190	0.298, 1.012 (H^γ)
84 Tyr	8.629	4.704	2.926, 3.407	7.133 (H^δ); 6.875 (H^ϵ)
85 Gly	7.606	4.351, 4.000		
86 Ile	7.608	4.375	1.776	0.856 ($H^{\gamma 2}$); 1.516, 1.156 ($H^{\gamma 1}$); 0.882 (H^δ)

[a] Measured in parts per million relative to the methyl group proton resonance of 4,4-dimethylsilapentane.

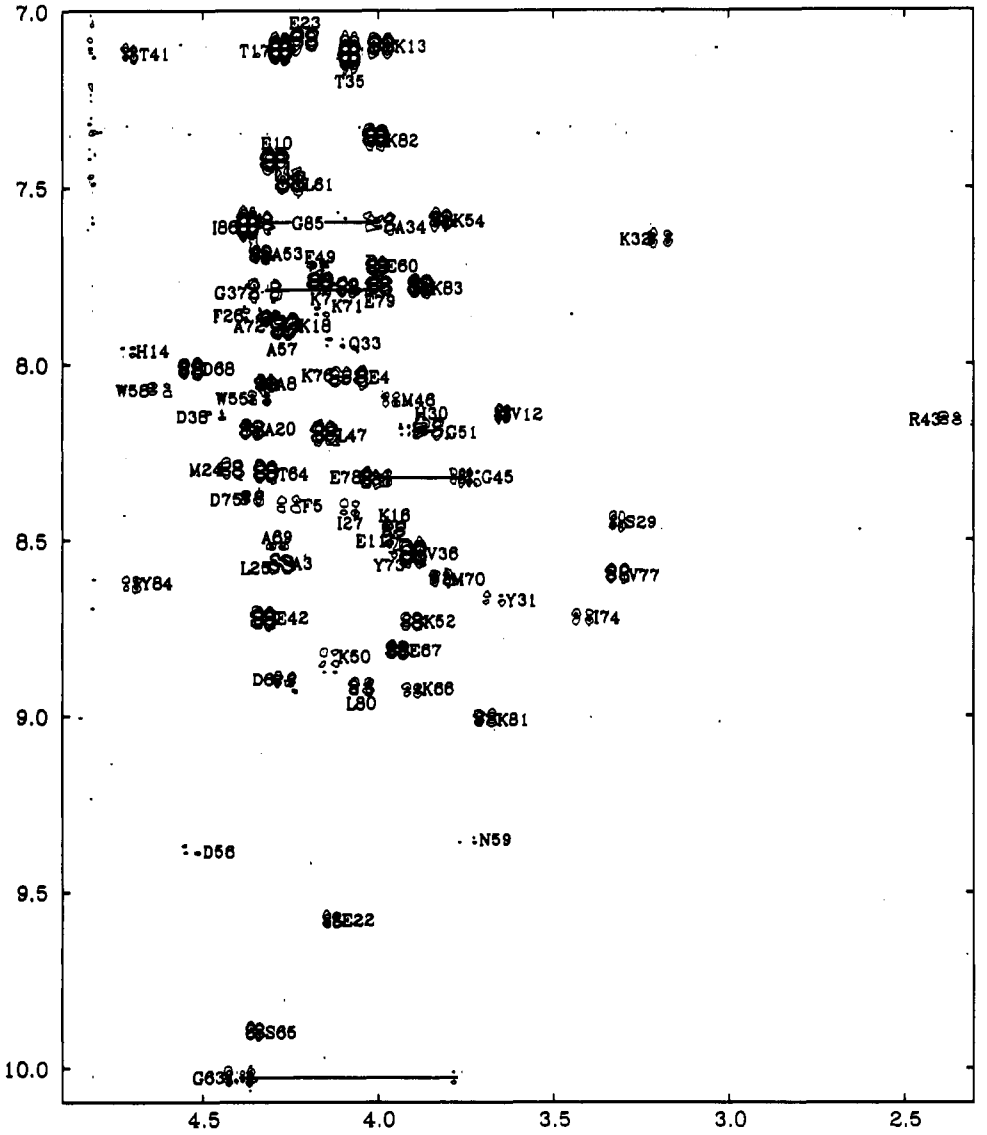

FIGURE 1: Fingerprint region of the DQF-COSY spectrum of recombinant ACBP 10 mM in 90:10 $H_2O/^2H_2O$, at pH 7.0 and 298 K. The cross peaks of residues Leu15, Asp21, Tyr28, and Lys62 are not visible at these contour levels. Residues Ala9 and Asn40 are not visible since their $C^\alpha H$ is at the water proton resonance. Residues Ser1, Gln2, Ile39, and Asp48 are not seen in this spectrum (see the text).

in which resonances of all protons were identified. The connectivity of the benzenoid part of the spin systems of the two tryptophans to the $H^{\epsilon 1}$ and the $H^{\delta 1}$ of the indole ring were in both cases obtained from the NOE effects between the $H^{\epsilon 1}$ and the $H^{\zeta 2}$. No differences in chemical shifts of the aromatic side-chain proton resonances between the recombinant and the native ACBP were observed. The connectivity between the aromatic and the aliphatic spin systems of these amino acids was obtained in all cases from the NOEs between the H^δs and the H^βs and in most cases also the H^α or the H^N of the spin systems (Figure 5). The chemical shifts of the AMX part of the aromatic residues were in all cases, except one, closely similar in the recombinant and the native ACBP. In Phe5 the chemical shifts of the H^α and one of the H^β were significantly different for the two proteins. In fact, the largest difference in chemical shifts observed between the two proteins was observed for the H^N of Phe5 being 0.39 ppm.

Histidines (His14 and His30). The two histidine spin systems were assigned in the recombinant ACBP (Figure 5); the $H^{\epsilon 1}$ of His30 has not been observed. In the native protein neither the imidazole nor the H^N–H^α spin system parts of His 14 were detected.

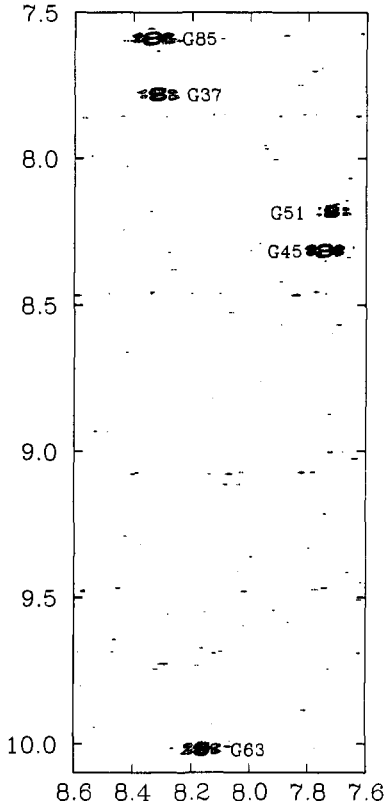

FIGURE 2: Expanded region of 2QS spectrum of recombinant ACBP (10 mM in 90:10 $H_2O/^2H_2O$, pH 7.0 and 298 K), showing the five NH–($C^{\alpha 1}H$ + $C^{\alpha 2}H$) cross peaks from the five glycines in ACBP.

AMX Systems (Ser1, Ser29, and Ser65; Asp21, Asp38, Asp48, Asp56, Asp61, Asp68, and Asp75; Asn40 and Asn59). The spin systems of the three serines were tentatively identified on the basis of the H^{β} chemical shifts that in all three spin systems were at lower field than those of the other AMX spin systems in the protein, but they were confirmed in the subsequent sequential assignment process. In the recombinant ACBP the N-terminal serine was clearly different from that of the native as expected due to the absence of N-acetylation. In the native ACBP the H^N of the acetylated N-terminal serine was identified. For Ser29 the H^{γ} of the hydroxy group, which is not normally seen in protein NMR spectra, was observed at 5.011 ppm in the spectra of the recombinant protein. Distinction of the aspartic and asparagine AMX systems from the pH dependance of the H^{β} chemical shifts was not possible given that the pH range of the studies was limited to the narrow pH range above the isoelectric point of the protein and above the p*K*s of their carboxylates. So, this distinction was mainly based on the identification of the $H^{\delta 21}$–$H^{\delta 22}$ coupling and the NOEs between these and the remaining protons of the spin systems of the two asparagines. Further evidence for these assignments was based mainly on the subsequent sequential assignment. The H^N–H^{α} cross peak of Asp48 was identified in a 2QS spectrum recorded without water suppression, and the spin system was identified by NOE effects from H^N to the H^{β}s. The assignment of all the AMX spin systems, including the aromatic amino acids and the histidines, identified the two H^{β} resonances at separate chemical shift positions. The H^N of Asp6 was shifted slightly downfield in the recombinant ACBP. The chemical shifts of the remaining asparagine and aspartate resonances were very similar in the spectra of the two proteins.

Glutamines (Gln2 and Gln33). The spin system of Gln2 like that of the N-terminal Ser1 was fully identified in the

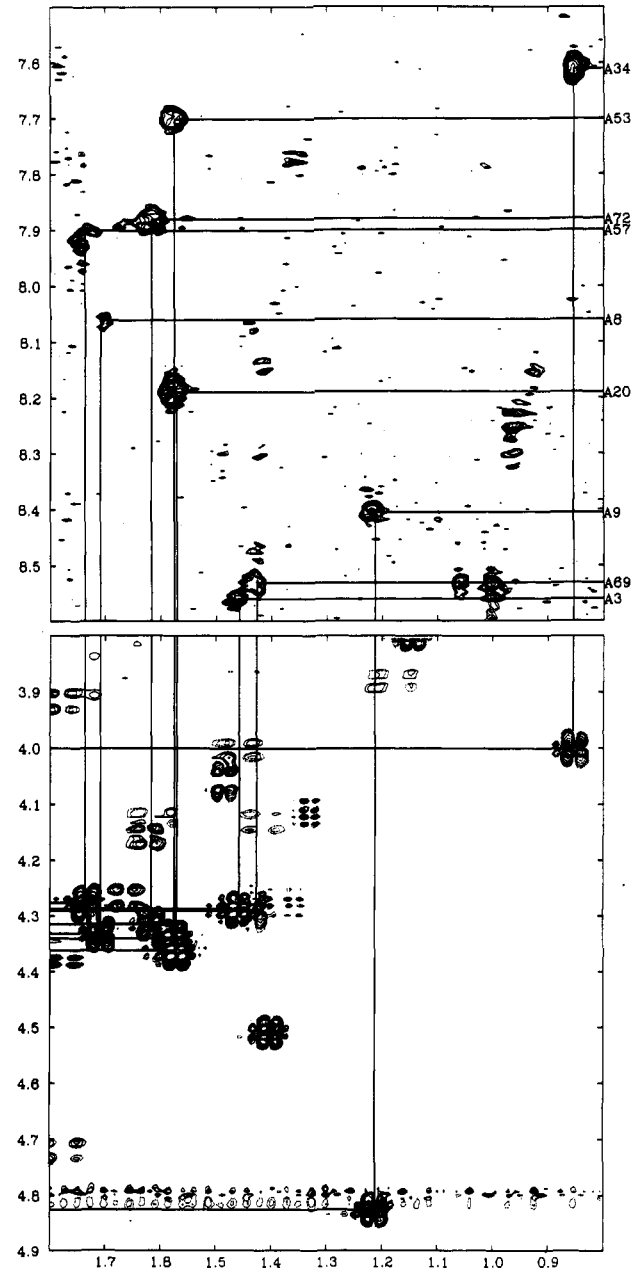

FIGURE 3: TOCSY (mixing time 65 ms, 10 mM in H_2O, pH 7.0 and 298 K) and DQF-COSY spectra of recombinant ACBP (10 mM in ^2H_2O, pH 7.0, and 298 K). The TOCSY spectrum (top) shows the H^N–H^{β} cross peaks of the nine alanines. The DQF-COSY spectrum (bottom) shows the H^{α}–H^{β} cross peaks of the alanines.

NMR spectra of the native ACBP, except for one H^{γ}, whereas in the recombinant ACBP only one H^{γ} and the two $H^{\epsilon 2}$ proton resonances were identified. For Gln33 resonances for only one H^{β} and one H^{γ} were observed.

Glutamates (Glu4, Glu10, Glu11, Glu22, Glu23, Glu42, Glu60, Glu67, Glu78, and Glu79), Methionines (Met25, Met46, and Met70), Prolines (Pro19 and Pro44), Lysines (Lys7, Lys13, Lys16, Lys18, Lys32, Lys50, Lys52, Lys54, Lys62, Lys66, Lys71, Lys76, Lys81, Lys82, and Lys83), and Arginines (Arg43). The full spin system assignment of these residue types that typically in other protein NMR studies have been difficult were accomplished only in the following cases: Glu11, Pro19, Met24, Lys32, Pro44, Met46, Met70, and Glu78. The assignment of Lys32 and Arg43 were both favored by very large ring current shifts of the resonances of their side-chain atoms. In most cases the assignment of these residue types were only possible for the H^N, H^{α}, and H^{β}.

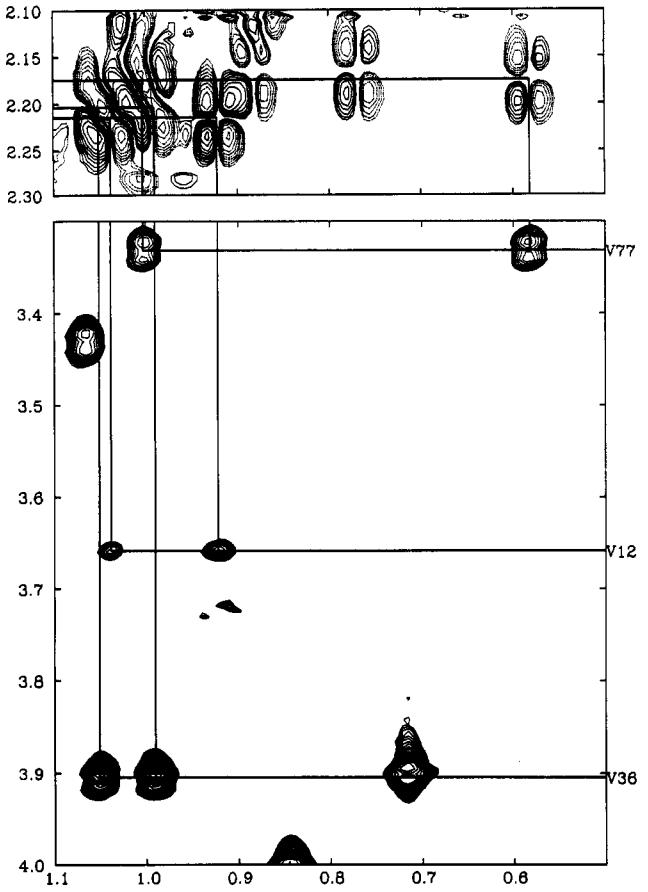

FIGURE 4: TOCSY (mixing time 65 ms) and DQF-COSY spectra of recombinant ACBP (10 mM in ^2H_2O, pH 7.0, and 298 K). The DQF-COSY spectrum (top) shows the H^{β}–H^{γ} cross peaks of the three valines. The TOCSY spectrum (bottom) shows the H^{α}–H^{γ} cross peaks of the valines.

Sequential Assignment

The sequential assignment was based on the NOESY spectra of the native and the recombinant ACBP, respectively, both recorded with mixing times of 50, 100, 150 and 200 ms. Four pieces of the amino acid sequence were assigned by the $d_{NN}(i,i+1)$ connectivities as shown in Figure 6a–d. These sequential connectivities were the most common in the spectra of the two proteins. The remaining part of the sequential assignment was established by the $d_{\alpha N}(i,i+1)$ and for sequences with proline in the $(i+1)$ position by the $d_{\alpha\delta}(i,i+1)$ connectivities; the exceptions being the peptide segment of Leu47 to Lys50, for which no sequential assignments were observed, and the connection from Thr41 to Glu42, which was determined by a $H^{\gamma 2}$–H^{N} NOE effect. The sequential assignments of the two residues Asp48 and Phe49 were, therefore, based on the elimination of other possibilities after the full sequential assignment of all the other amino acid spin systems in the protein. In addition to these three types of sequential NOEs, several other typical sequential NOEs were detected in the spectra. A summary of these is shown in Figure 7.

Secondary Structure

The combinations of sequential NOEs observed in the four stretches of the sequence 1–15, 22–35, 52–60, and 68–85 are all typical for those normally found in α-helices (Figure 7). The measurements of the $^3J_{H^N H^{\alpha}}$ (Figure 7) showed that the ϕ angle of the residues in these segments of the amino acid sequence were in the range around $-60°$ typical for α-helices. Accurate measurements of the coupling constants were, however, hampered by the line widths of approximately 10–16 Hz that were encountered for most of the residues.

The accurate start and end sequence positions of the helices proposed here cannot be determined unambiguously from the ACBP NOE data. For example, the beginning of α-helix 4 could well be at Glu67 given the $d_{\alpha N}(i,i+3)$ effect between this residue and Met70. In fact, the slow hydrogen exchange behavior of the residues Ala69, Met70, and Lys71 suggests that their amides are hydrogen bonded, and in that case the helix should start even at Ser65, provided the proposed hydrogen bondings do not involve other regions of the protein.

A qualitative estimate of the amide hydrogen solvent exchange revealed that only in the C-terminal α-helix a contiguous stretch of peptide sequence was characterized by slow amide exchange. As, however, these estimates were based on experiments recorded at pH 7.0 where amide hydrogen exchange is typically very fast, this observation only suggests that the most slowly exchanging amide hydrogens in the ACBP molecule are hydrogen bonded and protected from hydrogen exchange. The few positions of slow amide hydrogen exchange are otherwise typically found in regions of the peptide sequence that are α-helices according to the sequential assignment

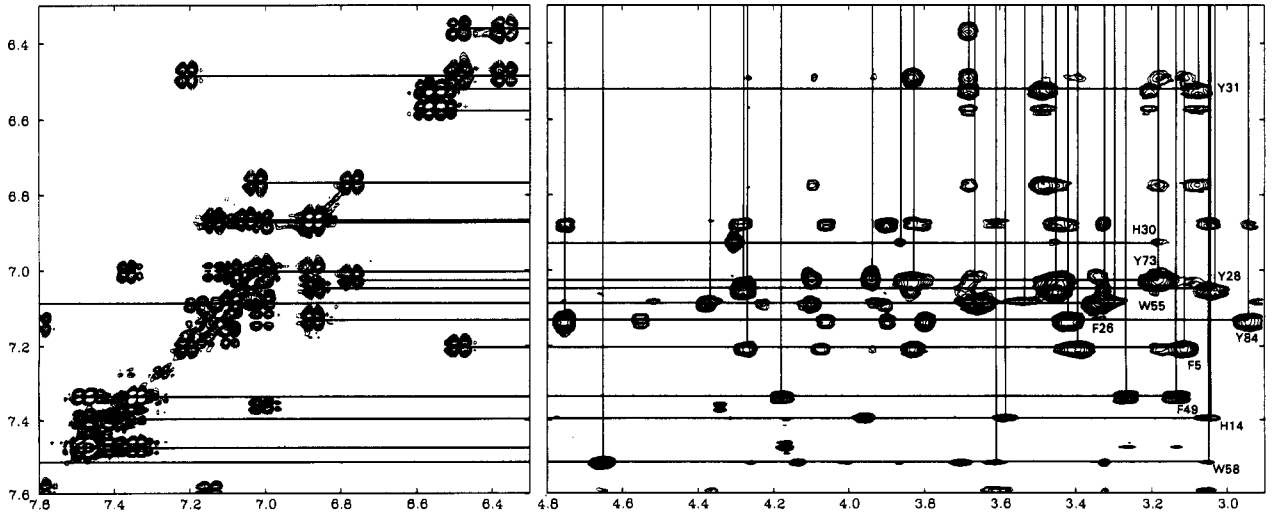

FIGURE 5: DQF-COSY spectrum recorded in H_2O and NOESY spectrum recorded in ^2H_2O of recombinant ACBP (10 mM, pH 7.0, and 298 K). The DQF-COSY spectrum (left) is a part of the aromatic region of the spectrum. The horizontal lines indicate the chemical shift positions of H^{δ}s of the aromatic residues of phenylalanines, tyrosines, and tryptophans and of the histidine residues.

Table II: ^{1}H Chemical Shifts ±0.002 in Native ACBP at pH 7.0 and 298 K[a]

residue	H^N	N^α	H^β	others
1 Ser	8.294[b]	4.597[c]	4.197, 4.001	
2 Gln	8.844[b]	3.953[b]	2.222,[b] 2.081[b]	2.431 (H^γ); 8.236, 6.562 ($H^{\epsilon 2}$)
3 Ala	8.481[c]	4.304	1.471	
4 Glu	7.918[c]	4.054	2.377, 2.377	
5 Phe	8.786[c]	4.213	3.380, 3.035	7.195 (H^δ); 6.488 (H^ϵ); 6.360 (H^ζ)
6 Asp	9.013[c]	4.278	2.779, 2.673	
8 Ala	8.131[c]	4.322	1.697	
9 Ala	8.477[c]	4.810	1.219	
29 Ser	8.503[c]	3.320		
67 Glu	8.905[c]	3.990		
70 Met	8.670[c]	3.845	2.191	2.473 (H^γ)
71 Lys	7.914[c]	4.075	2.059	1.610 (H^γ)

[a] Measured in parts per million as in Table I. Only residues which are not seen in recombinant ACBP and residues for which resonances are shifted more than 0.05 ppm are listed. [b] Protons not seen in recombinant ACBP. [c] Protons shifted more than 0.05 ppm relative to recombinant ACBP.

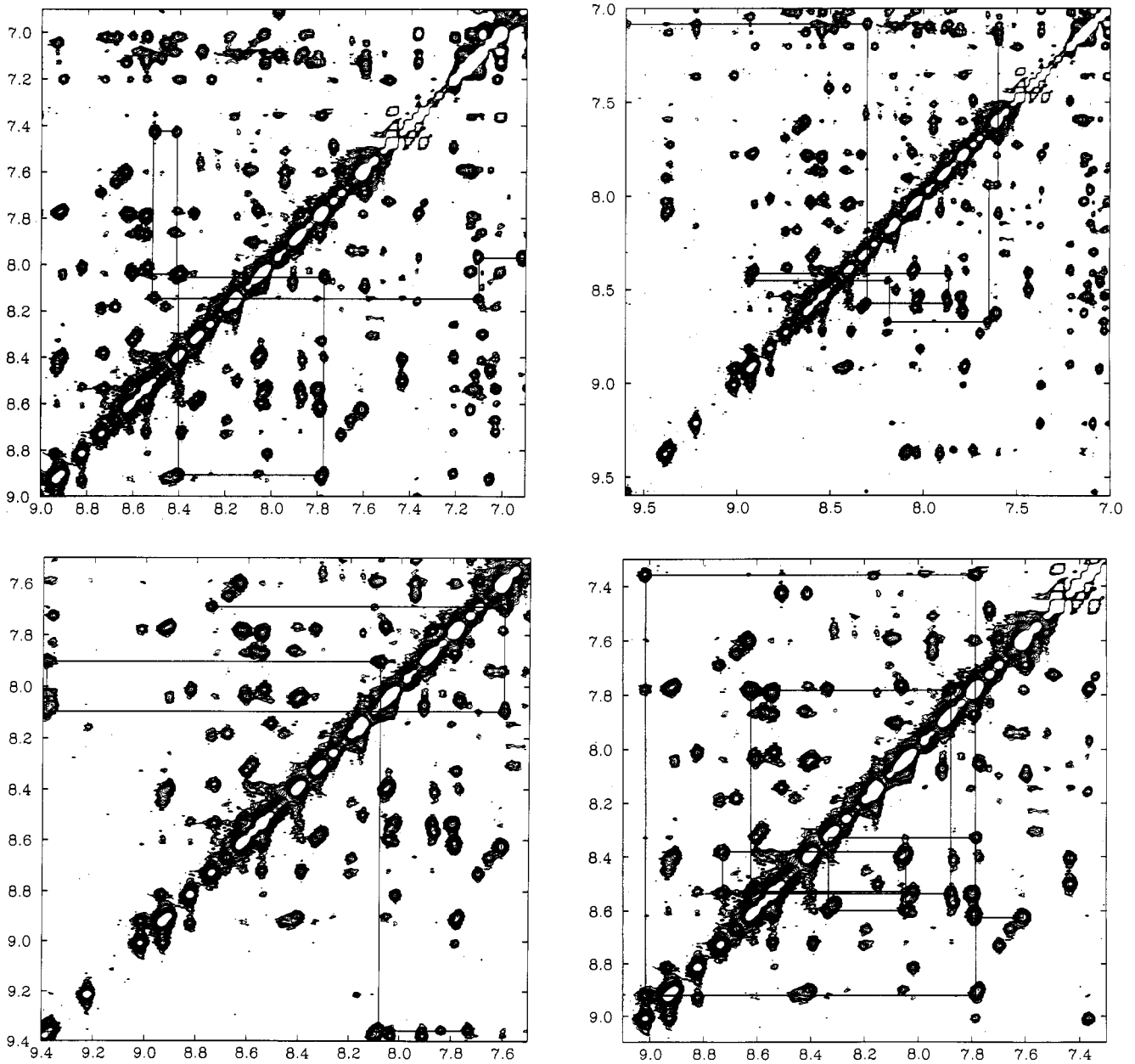

FIGURE 6: Expanded regions of the NOESY spectrum of recombinant ACBP (mixing time 200 ms, H_2O, pH 7.0, and 298 K), illustrating the assignment of the four α-helical regions via d_{NN} connectivities. (a, top left) Helix 1 (residues 3–15). (b, top right) Helix 2 (residues 22–35). (c, bottom left) Helix 3 (residues 52–60). (d, bottom right) Helix 4 (residues 68–85).

pattern. Exceptions, however, of slow amide exchange are observed at positions Val36, Gln60, and Thr64, which are all between the proposed α-helical segments, suggesting that they could be in stable reverse turn configurations. However, apart from the indications of amide hydrogen exchange sufficient evidence for turns in these positions has not been obtained.

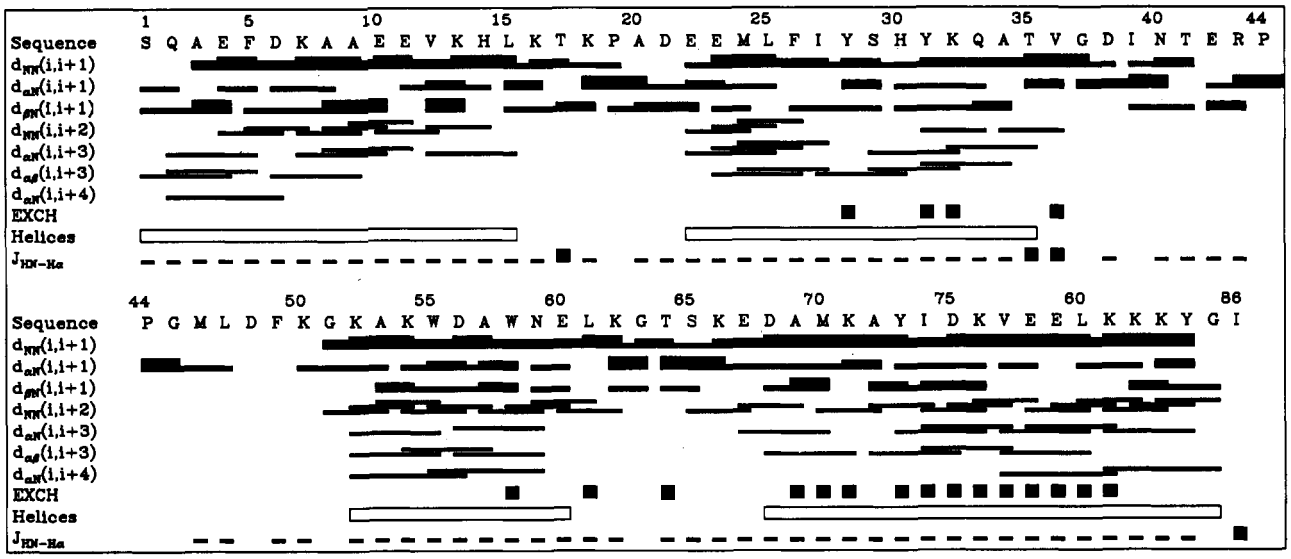

FIGURE 7: Summary of the sequential NOEs, amide proton exchange, and elements of secondary structure found in ACBP. NOEs are classified as either strong, medium, or weak distinguished by the thickness of the line. For prolines in the $(i+1)$ position, $d_{\alpha\delta}$ are shown in the $d_{\alpha N}$ row. Amide proton exchange is classified as slow by a thick line. α-Helical regions are indicated by open boxes. Coupling constants $^3J_{H^NH^\alpha} < 7$ Hz are represented by a thin line, and those >8 Hz are represented by a thick line.

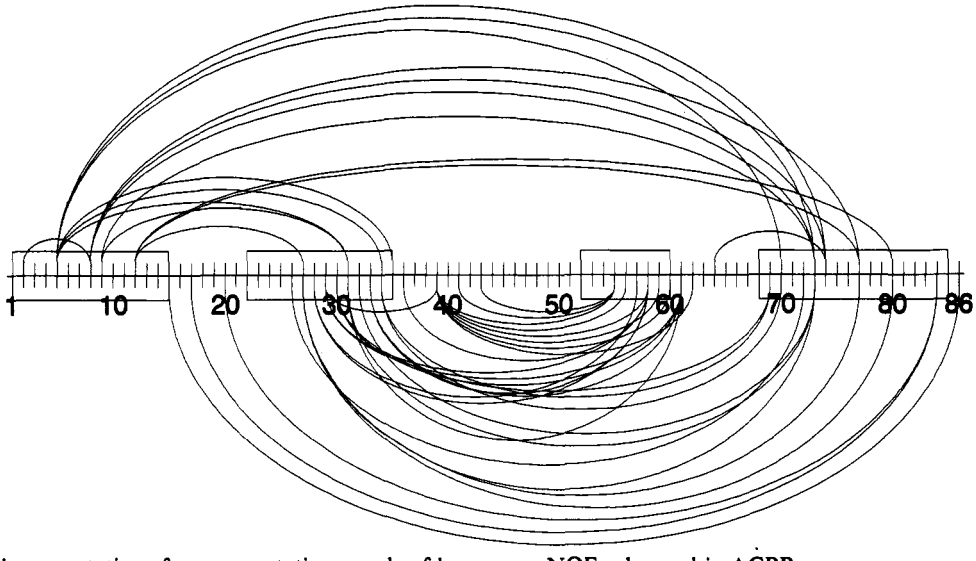

FIGURE 8: Schematic presentation of a representative sample of long-range NOEs observed in ACBP.

DISCUSSION

The sequence-specific assignment of both ACBP and recombinant ACBP has resulted in assignments of many complete sequentially assigned spin systems, as well as in a fairly large number of fragmentary but sequentially assigned spin systems. These latter, in particular, were of residues typically present on the surface of protein molecules, for example, glutamates and lysines, that account for 24 of the 86 amino acid residues of ACBP. The sequential assignment, however, has made it possible to investigate the secondary structure of the two proteins. The sequential NOEs and the measured coupling constants observed in the spectra of both molecules are qualitatively very similar. This suggests, not surprisingly, that the two protein molecules are very similar with respect to their secondary structure. Despite the difficulties encountered in precise determination of the start and end of the helices, it remains very clear that the ACBP is a four α-helix protein.

A full protein structure determination of ACBP is presently in progress, and evidence is already available at this stage that allows the drawing of an outline of the internal organization of the four α-helices. In Figure 8 a schematic presentation of a representative sample of the long-range NOEs is shown. This information, together with the information in Table II concerning shifts in recombinant ACBP relative to native ACBP, has made it possible to construct a model of the folded protein. The chemical shift differences in Table II between native and recombinant ACBP indicate that the N-terminal of helix 4 is close to the N-terminal of helix 1, and together with the long-range NOEs, which show contacts between Glu11 and Leu80, we have suggested that helix 1 and helix 4 are organized in a manner so that the axes of the helices in the direction from the N-terminal to the C-terminal are close to parallel. The long-range NOEs further suggest that helix 2 in these terms is close to antiparallel to helix 1 and helix 4. The position of helix 3 is more uncertain. From helix 3 there are only long-range NOEs to helix 2 (none to helix 1 and 4), indicating that helix 2 is placed between helix 3 and the substructure of helix 1 and 4. The nonhelical segment between helix 3 and helix 4 is only seven residues, and since the N-terminal of helix 4 has NOEs to the C-terminal of helix 2, this

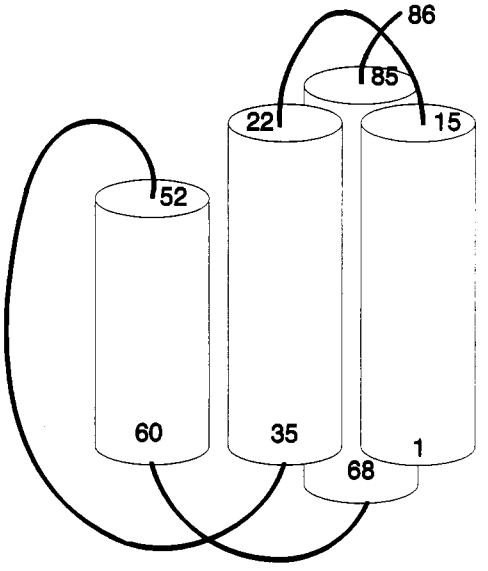

FIGURE 9: Schematic diagram of possible global fold. The four helices are depicted as cylinders and the remaining protein sequence as thick lines.

suggests that the C-terminal of helix 3 is close to the C-terminal of helix 4, and therefore the structure can be arranged so that helix 2 and 3 are approximately parallel. The nonhelical part of the protein has only a few long-range NOEs, suggesting that the residues in these parts have few nonpolar contacts with the four helices. The residues between sequence postions 44 and 51 form the longest nonhelical stretch in the sequence with no long-range NOEs, suggesting that this region of the structure is a loop. Figure 9 summarizes this in a schematic form.

The assignment presented in this paper will provide the basis for further calculations of the three-dimensional structure of ACBP.

ACKNOWLEDGMENTS

We thank Rikke Sørensen, Erling Knudsen, and Pia Mikkelsen for skilled technical assistance and Mogens Kjær for advice and help with computations.

REFERENCES

Anil-Kumar, Ernst, R. R., & Wüthrich, K. (1980) A Two-Dimensional Nuclear Overhauser Enhancement (2D NOE) Experiment for the Elucidation of Complete Proton–Proton Cross-Relaxation Networks in Biological Macromolecules, *Biochem. Biophys. Res. Commun. 95*, 1–5.

Anil-Kumar, Wagner, G., Ernst, R. R., & Wüthrich, K. (1981) Buildup Rates of the Nuclear Overhauser Effect Measured by Two-Dimensional Proton Magnetic Resonance Spectroscopy: Implication for Studies of Protein Conformation, *J. Am. Chem. Soc. 103*, 3654–3658.

Aue, W. P., Bartholdi, E., & Ernst, R. R. (1976) Two-Dimentional Spectroscopy. Application to Nuclear Magnetic Resonance, *J. Chem. Phys. 64*, 2229–2246.

Bachmann, P., Aue, W. P., Müller, L., & Ernst, R. R. (1977) Phase Separation in Two-Dimensional Spectroscopy, *J. Magn. Reson. 28*, 29–39.

Bax, A., & Davis, D. G. (1985) Practical Aspects of Two-Dimensional Transverse NOE Spectroscopy, *J. Magn. Reson. 65*, 355–360.

Besman, M. J., Yanagibashi, K., Lee, T. D., Kawamura, M., Hall, P. F., & Shively, J. E. (1989) Identification of Des-(Gly-Ile)-endozepine as an Effector of Corticotropin-Dependent Adrenal Steroidogenesis: Stimulation of Cholesterol Delivery Is Mediated by Peripheral Benzodiazepine Receptor, *Proc. Natl. Acad. Sci. U.S.A. 86*, 4897–4901.

Boyd, J., Dobson, C. M., & Redfield, C. (1983) Correlation of Proton Chemical Shift Using Two-Dimensional Double-Quantum Spectroscopy, *J. Magn. Reson. 55*, 170–176.

Braunschweiler, L., & Ernst, R. R. (1983) Coherence Transfer by Isotropic Mixing: Application to Proton Correlation Spectroscopy, *J. Magn. Reson. 53*, 521–528.

Braunschweiler, L., Bodenhausen, G., & Ernst, R. R. (1983) Analysis of Networks of Coupled Spins by Multiple Quantum NMR, *Mol. Phys. 48*, 535–560.

Chen, Z. W., Agerberth, B., Gell, K., Anderson, M., Mutt, V., Östenson, C. G., Efendic, S., Barros-Söderling, J., Persson, B., & Jörnvall, H. (1988) Isolation and Characterization of Porcine Diazepam-Binging Inhibitor, a Polypeptide not only of Cerebral Occurrence but also Common in Intestinal Tissues and with Effect on Regulation of Insulin Release, *Eur. J. Biochem. 174*, 239–245.

Eich, G., Bodenhausen, G., & Ernst, R. R. (1982) Exploring Nuclear Spin Systems by Relayed Magnetization Transfer, *J. Am. Chem. Soc. 104*, 3731–3732.

Griesinger, C., Otting, G., Wüthrich, K., & Ernst, R. R. (1988) Clean TOCSY for ^{1}H Spin System Identification in Macromolecules, *J. Am. Chem. Soc. 110*, 7870–7872.

Jeener J., Meier, B. H., Bachmann, P., & Ernst, R. R. (1979) Investigation of Exchange Processes by Two-Dimensional NMR Spectroscopy, *J. Chem. Phys. 71*, 4546–4553.

Kjær, M., Ludvigsen, S., Sørensen, O. W., Denys, L. A., Kindtler, J., & Poulsen, F. M. (1987) Sequence Specific Assignment of the Proton Nuclear Magnetic Resonance Spectrum of Barley Serine Proteinase Inhibitor 2, *Carlsberg Res. Commun. 52*, 327–354.

Kjær, M., Andersen, K. V., Shen, H., Ludvigsen, S., Vindekilde, D., Sørensen, B., & Poulsen, F. M. (1991) *Outline of a Computer Program for the Analysis* of *Protein NMR Spectra.* (Hoch, J. C., Redfield, C., & Poulsen, F. M., Eds.) NATO ASI series, Plenum, New York.

Knudsen, J. (1991) Acyl-CoA Binding and Transport. An Alternative Function for Diazepam Binding Inhibitor (DBI) Which Is Identical with Acyl-CoA-Binding Protein (ACBP), *Neuropharmacology* (in press).

Knudsen, J., & Nielsen, M. (1990) Diazepam Binding Inhibitor: A Neuropeptide and/or an Acyl-CoA Ester Binding Protein?, *Biochem. J. 265*, 927–929.

Ludvigsen, S., Andersen, K. V., & Poulsen, F. M. (1991) Accurate Measurements of Coupling Constants from Two-Dimensional NMR Spectra of Proteins and Determination of ϕ Angles, *J. Mol. Biol. 217*, 731–736.

Marion, D., & Wüthrich, K. (1983) Application of Phase Sensitive Two-Dimensional NMR Spectroscopy, *Biochem. Biophys. Res. Commun. 113*, 967–974.

Mandrup, S., Højrup, P., Kristiansen, K., & Knudsen, J. (1991) Gene Synthesis, Expression in *E. coli*, Purification and Characterization of the Recombinant Bovine Acyl-CoA Binding Protein (ACBP), *Biochem. J. 276*, 817–823.

Mikkelsen, J., Højrup, P., Nielsen, P. F., Roepstorff, P., & Knudsen, J. (1987) Amino Acid sequence of acyl-CoA-binding protein from cow liver, *Biochem. J. 245*, 859–861.

Mogensen, I. B., Schulenberg, H., Hansen, H. O., Spener, F., & Knudsen, J. (1987) A novel acyl-CoA binding protein from bovine liver. Effect on fatty acid synthesis, *Biochem. J. 241*, 189–192.

Neuhaus, D., Wagner, G., Vašák, M., Kägi, J. H. R., & Wüthrich, K. (1985) Systematic Application of High

Resolution Phase-Sensitive Two-Dimensional ^{1}H NMR Techniques for the Identification of the Amino-Acid-Proton Spin Systems in Proteins. Rabbit Metallothionein-2, *Eur. J. Biochem. 151*, 257–273.
Piantini, U., Sørensen, O. W., & Ernst, R. R. (1982) Multiple Quantum Filters for Elucidating NMR Coupling Networks, *J. Am. Chem. Soc. 104*, 6800–6801.
Rance, M., Sørensen, O. W., Bodenhausen, G., Wagner, G., Ernst, R. R., & Wüthrich, K. (1983) Improved Spectral Resolution of COSY ^{1}H NMR Spectra of Proteins via Double Quantum Filtering, *Biochem. Biophys. Res. Commun. 117*, 479–485.
Rasmussen, J. T., Börchers, T., & Knudsen, J. (1990) Comparison of the Binding Affinities of Acyl-CoA-Binding Protein (ACBP) and Fatty Acid-Binding Protein for Long Chain Acyl–CoA Esters, *Biochem. J. 265*, 849–855.
States, D. J., Haberkorn, R. A., & Ruben, D. J. (1982) A Two-Dimensional Nuclear Overhauser Experiment with Pure Absorption Phase in Four Quadrants, *J. Magn. Reson. 48*, 286–292.
Wagner, G. (1983) Two-Dimensional Relayed Coherence Transfer Spectroscopy of a Protein, *J. Magn.* Reson. *55*, 151–156.
Wagner, G., & Zuiderweg, E. R. P. (1983) Two-Dimensional Double Quantum ^{1}H NMR Spectroscopy of Proteins, *Biochem. Biophys. Res.* Commun. *113*, 854–860.
Wüthrich, K. (1986) *NMR of Proteins and Nucleic Acids*, Wiley, New York.

Yeast 6-Phosphofructo-2-kinase: Sequence and Mutant[†,‡]

Matthias Kretschmer and Dan G. Fraenkel*
Department of Microbiology and Molecular Genetics, Harvard Medical School, Boston, Massachusetts 02115
Received April 29, 1991; Revised Manuscript Received July 15, 1991

ABSTRACT: We have reported yeast 6-phosphofructo-2-kinase (EC 2.7.1.105) as having a ca. 96-kDa subunit size, as well as isolation of its structural gene, *PFK26*. Sequencing now shows an open reading frame of 827 amino acids and 93.5 kDa. The deduced amino acid sequence has 42% identity with the 55-kDa subunit of the bifunctional 6-phosphofructo-2-kinase/fructose-2,6-bisphosphatase from rat liver with extra material at both ends. Although the yeast sequence is especially similar to the liver one in its bisphosphatase domain, the essential His-258 of the liver enzyme is, in yeast, a serine, which may explain the apparent lack of bisphosphatase activity. Also, the yeast enzyme, known to be activated via protein kinase A, has a putative phosphorylation site near its C-terminus and lacks the N-terminal phosphorylation sequence involved in inhibition of the liver enzyme. In a chromosomal null mutant strain, *pfk26*::*LEU2*, activity was marginal and the protein was not detectable as antigen. The mutant strain grew well on glucose and contained a near-normal level of fructose 2,6-P_2. But in its growth on pyruvate, by contrast with the wild-type strain, no fructose 2,6-P_2 was detectable, and it did not form after glucose addition in the presence of cycloheximide either. Such resting cells, however, metabolized glucose at the normal high rate. Glucose addition to the *pfk26* mutant strain in the absence of cycloheximide, on the other hand, caused a ca. 10% normal rate of fructose 2,6-P_2 accumulation, presumably employing a glucose-inducible second enzyme. Using strains also lacking 6-phosphofructo-1-kinase, affinity chromatography revealed the second enzyme as a minor peak amounting to 6% of 6-phosphofructo-2-kinase activity in a *PFK26* strain and as the sole peak, in similar amount, in a *pfk26* mutant strain.

Fructose 2,6-bisphosphate (fructose 2,6-P_2) has a major role in carbohydrate metabolism in higher cells as activator of 6-phosphofructo-1-kinase (EC 2.7.1.11) and inhibitor of fructose-1,6-bisphosphatase (EC 3.1.3.11) (Hers, 1984). It is formed from fructose 6-P and ATP by 6-phosphofructo-2-kinase (EC 2.7.1.105) and hydrolyzed to fructose 6-P and P_i by fructose-2,6-bisphosphatase (EC 3.1.3.46) (Pilkis et al., 1987). In liver, muscle, and heart, both activities reside on a bifunctional protein of low specific activity; in liver this enzyme is subject to cAMP-dependent phosphorylation, which causes inhibition of the kinase and activation of the phosphatase activities (Van Schaftingen & Hers, 1982).

Saccharomyces cerevisiae also contains fructose 2,6-P_2, an activator in vitro of its 6-phosphofructo-1-kinase and inhibitor of its fructose 1,6-bisphosphatase (Kessler et al., 1988; Lederer et al., 1981; Clifton & Fraenkel, 1983). 6-Phosphofructo-2-kinase in yeast differs from the mammalian enzymes in apparently not being bifunctional (François et al., 1988; Kretschmer et al., 1987), having a larger subunit size (96 kDa instead of 55 kDa), likely having a much higher catalytic rate, and being present in minute amount ($<10^{-5}$ of cell protein) (Kretschmer et al., 1991). Also, the yeast enzyme is activated by protein kinase A (François et al., 1988), in this respect resembling the enzyme from heart (Sakata et al., 1990). Cloning employed mixed oligonucleotide probes to tryptic peptide sequences, and the gene in multicopy overproduced both enzyme activity and antigen (Kretschmer et al., 1991).

Here we describe (i) the DNA sequence coding for this gene (*PFK26*), (ii) a chromosomal deletion mutant, (iii) a situation of rapid glucose metabolism in the absence of fructose 2,6-P_2, and (iv) evidence for a second, minor, 6-phosphofructo-2-kinase activity apparently induced in growth on glucose.

Materials and Methods

Materials. Fructose 6-P, ATP, and most enzymes were from Boehringer (Mannheim, Germany). Fructose 2,6-P_2,

[†]Supported by NIH Grant GM21098.
[‡]The nucleotide sequence reported in this paper has been submitted to GenBank under Accession Number J05351.

0006-2960/91/0430-10663$02.50/0 © 1991 American Chemical Society